DESIGN AND EXPLORATION OF FEEDFORWARD HAPTIC FEEDBACK IN ANTHROPOMORPHICALLY-DRIVEN PROSTHESES

by

Ethan D. Miller

An essay submitted to The Johns Hopkins University in conformity with the requirements for the degree of Master of Science in Engineering.

Baltimore, Maryland

May, 2020

Abstract

Here, we present a wearable, anthropomorphically-driven prosthesis with a built-in haptic feedback system. The device was designed and built to accommodate specific design parameters. Two control schemes were proposed and compared in a user study with N=6 able-bodied participants performing the Box and Blocks test. The first control scheme was designed to provide an intuitive, human-like actuation and relaxation of the hand, while the other controller was designed to reduce fatigue from sustaining EMG signals. Participants performed significantly better with lower fatigue levels while using the intuitive controller as opposed to the second controller. In addition, task performance with both controllers was better than reported performance with standard myoelectric prostheses. In addition, a second experiment compared the unilateral manual dexterity of N=3 able-bodied participants under three distinct conditions: vibration haptic feedback, skin stretch haptic feedback, and no haptic feedback. These findings suggest that there is utility in wearable anthropomorphically-driven prostheses, and provide support for future studies aimed at exploring anthropomorphically-driven prostheses.

Thesis Committee

Jeremy Brown, PhD (Primary Advisor)

Assistant Professor

Department of Mechanical Engineering

Johns Hopkins Whiting School of Engineering

Gene Fridman, PhD

Associate Professor

Department of Otolaryngology Head and Neck Surgery, Biomedical Engineering, and Electrical and Computer Engineering

Johns Hopkins Whiting School of Engineering and Johns Hopkins School of Medicine

Marlís Gonzalez-Fernandez, MD, PhD

Associate Professor

Department of Physical Medicine and Rehabilitation

Johns Hopkins School of Medicine

Acknowledgments

I would like to thank Dr. Jeremy Brown and Ihemriorochi Amanze for joining me and supporting me in this work. I would also like to thank Dankmeyer, Inc. for casting the custom socket and providing the Hosmer Quick Disconnect. I would also like to thank Maya Sitaram, Mohit Singhala, Sergio Machaca, Neha Thomas, and Garret Ung for their support and help throughout the project.

Dedication

To all those who believed in me

Know,

You have made my dreams reality

To Caitlin, for her unwavering support and confidence in me, which far surpasses my own. She has shown me I have more in me than I ever knew.

To my parents for letting me grow and explore the world around me with relentless encouragement for my curiosity.

To all my other parents for always loving me as their own and inspiring me.

To my siblings for showing me the way and for always exploring with me.

To my friends for their constant encouragement and guidance.

To my many mentors and teachers for their knowledge, time, care, commitment, encouragement, and passion.

Thank you.

Contents

List of Tables

List of Figures

Chapter 1

Introduction

There are nearly two million people in the United States living with an amputation. Of these, roughly 30% involve amputation of the upper extremity [1, 2]. Currently, the standard of care is to fit these amputees with a prosthesis that utilizes body-power or electromyography to control movement of the prosthetic terminal device (hand). While body-powered terminal devices are typically limited to single-DoF actuation of two digits, advanced myoelectric terminal devices, such as the i-Limb Ultra Revolution or the Michelangelo Hand, allow for multiple grip paradigms involving all five digits in a manner that mimics the natural hand [1]. A figure of these modern prostheses is provided in Fig. 1.1

i-Limb Be-bionic Michelangelo

Figure 1.1: A figure of the most advanced commercially available prostheses from [3]

1.0.1 Devices

Although these commercially available myoelectric terminal devices are designed to provide amputees with prostheses that emulate the form, function, and dexterity of an intact human hand [3, 4], they often feature actuation schemes with high gear-ratios that limit an amputee's ability to modulate the hand's impedance. Yet, it is widely accepted that humans modulate the impedance of their limbs for various tasks [5, 6]. There is even evidence to suggest that prosthesis users would modulate their device impedance for different tasks if allowed [7]. As a preliminary example, Brown *et al*. found that low-impedance prosthetic terminal devices allow grip/load force coordination in a manner consonant with the natural hand [8].

In an effort to allow control over the terminal device's impedance and to support more dexterous grasping movements, some experimental upper-limb prostheses use anthropomorphic actuation schemes [9–11]. Note that anthropomorphically-driven prostheses differ from other tendon driven prostheses, such as that used by Battaglia *et al*. [12], by allowing independent control over antagonistic tendons.

Modeled after grasping functions of the human hand [10], these anthropomorphically-driven hands utilize complex structures and many individualized actuators to flex and extend the hand. Typically in these devices, each finger has artificial ligaments and tendons that mimic the anterior and posterior structure of the human hand. Xu *et al*. , for example, demonstrated that their biomimetic anthropomorphically-driven robotic hand was capable of reliable, human like, finger movements that endowed their hand with the ability to grasp a variety of objects [11]. Unfortunately, in order to achieve higher dexterity than commercially available prostheses, many of these anthropomorphically-driven hands use large and bulky actuation systems, making them unwearable [13]. This limits the range of tasks with which these devices can be tested.

Despite their novel control schemes, these anthropomorphic devices are no different than commercial prostheses in terms of haptic sensory feedback. In the natural hand, haptic feedback is necessary for fine dexterous control [14–18]. When antagonist muscles are actuated, the information about tension can be used to interpret the state of the hand [19]. The need for haptic information about antagonistic tensions is therefore unique to anthropomorphically-driven hands [14]. While there is evidence to suggest this information could provide utility in prosthesis control [14], there is a lack of research assessing the performance effects of tension feedback in the control of anthropomorphically-driven prostheses. As prostheses develop and use more complex control schemes, such as brain machine interfaces,

it will be important to have a better understanding of the utility of various forms of haptic feedback.

1.0.2 Control modalities

The most common control methods for modern prostheses are electromyography (commonly referred to as myoelectric) and body-power. Body-powered prostheses allow for high fidelity control over a relatively simple terminal device. Additionally, body-powered control maintains the direct mechanical linkage between the user and the terminal device allowing for haptic feedback of tension, force, and aperture to be transmitted directly to the user.

On the other hand, myoelectric control provides a less physically cumbersome control approach over the prosthesis. More so, myoelectric prostheses typically provide stronger grip forces than body powered prostheses [20]. Additionally, myoelectric control allows for control over various grip patterns and various actuators. Despite these advantages, myoelectric control can be difficult and time consuming to learn. Despite the intricacy of myoelectric it will likely never be able to fully control anthropomorphically-driven prostheses to their fullest extent [21]. This control method also lacks the mechanical linkage that provides direct haptic feedback for the user. There is great debate over which, if either, myoelectric or body powered prostheses are better overall [20]. Each has clear advantages and disadvantages that must be considered as new prostheses are developed.

Beyond commercially available devices, there are other research devices that offer a more integrated control scheme. More prominent research control devices include targeted muscle reinnervation (TMR), peripheral nerve interfaces (PNI), and brain machine interfaces (BMI). TMR is a control strategy where damaged axons from an amputee's residual limb are surgically reinnervated into new muscles [22] to allow for heightened EMG control [23]. In addition, TMR has the added benifit of reducing phantom limb pain, or nerve pain caused from limb loss [22]. PNI controllers are a more invasive form of control that use implanted electrodes into the users peripheral nervous system in order to gain higher density and precision signals directly from the nervous system [24]. This direct connection has also allowed for sensory information to be relayed back to the prosthesis user [25]. Despite the high level of control provided, the long term viability of PNI controllers is currently unstable and requires more innovation to become a safe and effective control method for prosthesis users [26]. BMI are used to control a neuroprostheses by connecting directly to the brain [27–30]. Devices such as the USEA shown implanted peripherally in Fig.1.2 from Wendelken *et al*. 's work can provide multi-degree of freedom control over a virtual prosthesis [31–33]. These interfaces could allow for higher fidelity control over more actuators. They even offer the ability to provide various forms of haptic feedback directly to the user's brain [31, 34, 35]. While these devices are not yet viable as a long term solution to the control of prostheses, they are developing rapidly.

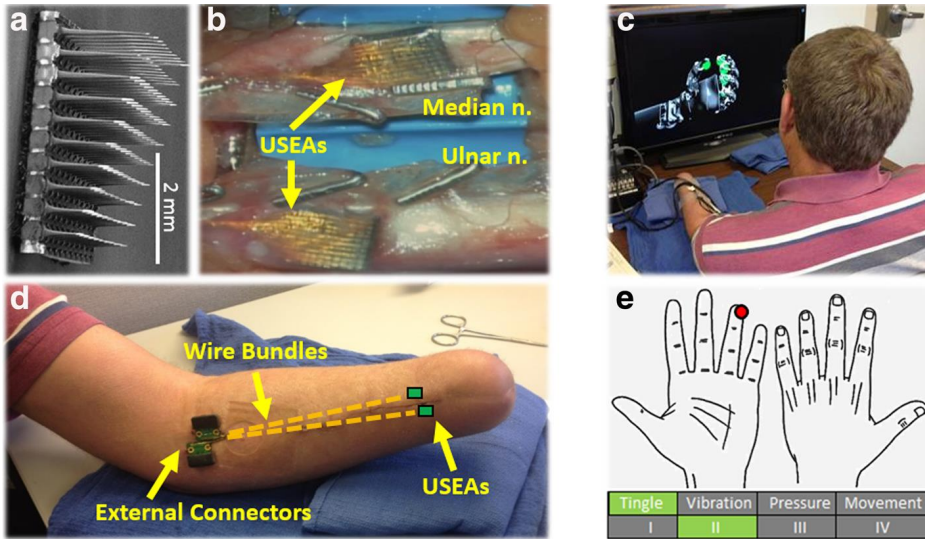

Figure 1.2: A figure of the USEA controller and the experimental set up from [31]

It is therefore important to understand the utility of haptic feedback in anthropomorphically-driven prostheses given the highlighted advancements in both prosthesis design and prosthesis control. To conduct these investigations, a wearable anthropomorphically-driven prosthesis was designed, built, and tested. Using this experimental apparatus, a number of studies were devised to investigate to what extent haptic feedback of the actuator improves user effectiveness, efficiency, and human-device integration. Overall, we hypothesize that providing haptic feedback of the actuator tension will improve user effectiveness, efficiency, and human-device integration. In the following chapters, I describe the design of the prosthesis and the methods used in the two experiments. Results for each experiment are also given and a discussion of the work is provided.

Chapter 2

Experimental Device Design

After exploring the current state of anthropomorphically-driven prostheses, it was apparent that there was a lack of experimentation involving utility from a user standpoint as well as a lack of haptic feedback research for these devices. From that conclusion it became evident that a unique anthropomorphically-driven prosthesis would need to be designed and tested. In addition, this is an opportunity to explore various forms of haptic feedback in anthropomorphically driven prostheses. Our experimental device, an anthropomorphically-driven prosthesis, was designed to incorporate two key features aimed at improving overall prosthesis functionality. First, the prosthesis features an anthropomorphic actuation paradigm that utilizes antagonistic tendons to separately control terminal device flexion and extension. Second, the prosthesis incorporates a unique haptic feedback system that utilizes skin-stretch to provide intuitive feedback regarding the amount of tension in either

tendon.

2.0.1 Device Design

2.0.1.1 Prosthesis Design

This anthropomorphically-driven prosthesis (see Fig. 2.1) is comprised of a custom co-polymer prosthesis socket mated to an anthropomorphic terminal device via a Hosmer Quick Disconnect Wrist (USMC model). The custom socket is designed to be worn by able-bodied individuals on their right arm. The goal in designing an anthropomorphically driven hand was to model the design after other anthropomorphic prostheses such as that designed by Atasoy *et al*. [36] or Xu *et al*. [10]. The anthropomorphic terminal device build here is based on the open source bionic hand originally designed by Hendo [37]. Modifications have been made to improve cable routing through the fingers and allow mating' compatibility with the Hosmer Quick Disconnect Wrist. The rubber bands on the anterior side of the original design were replaced with more tendon cabling to allow control over both flexion and extension. Each tendon cable originates at the finger tip, runs through the cable guides along the anterior and posterior sides of each finger, passes through the wrist cable guide, and terminates at a compression spring, which helps return the tendon cable to its resting position. Silicon (Smooth-On Inc, Dragon Skin 20) fingertips were designed for each finger to approximate the

size of a human finger. All tendon cables connect to the far end of either the anterior or posterior compression spring, simplifying the actuation of the device to flexion and/or extension of all fingers simultaneously. In addition, actuation of both anterior and posterior tendons creates a bidirectional impedance of variable magnitude. An actuator tendon cable connects a compression spring to a rotary DC motor (Maxon RE30). The motors are mounted on the proximal end of the socket through two custom 3D printed motor mounts. Each motor features a rotary optical encoder (US Digital, 5000 CPR) to measure motor rotation.

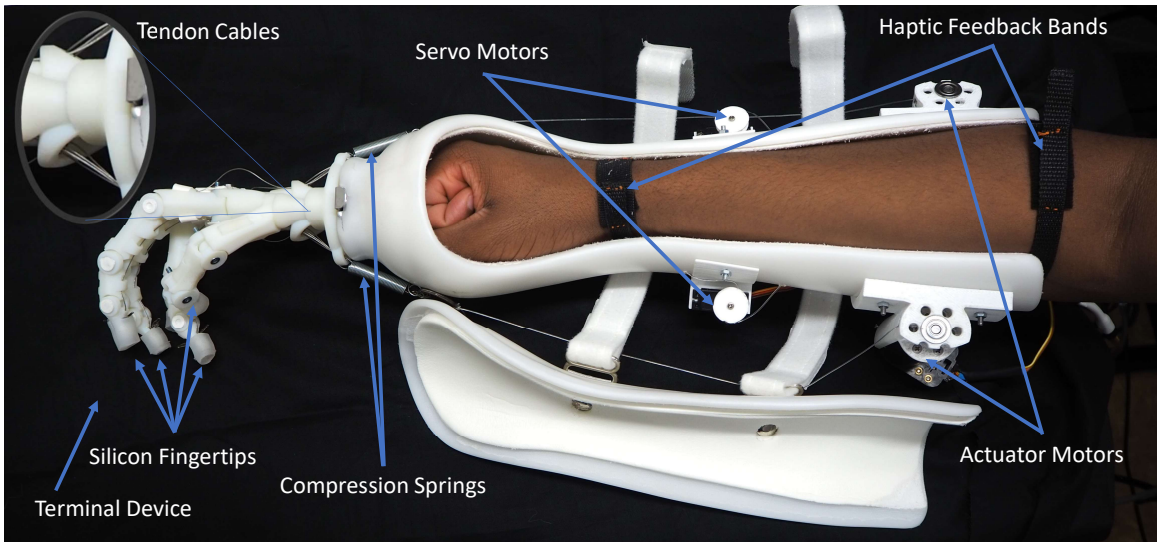

Figure 2.1: The anthropomorphically-driven prosthesis with the cover removed to show the haptic feedback bands around the user's forearm © 2020 IEEE.

2.0.1.2 Built in Hapics design

The built-in haptic feedback system is based on the design originally proposed by Kayhan *et al*. [38] and has been integrated into the co-polymer socket. The

haptic feedback system uses two servo motors (Tower Pro Micro servos MG90S) to create a pulling actuation on a proximal and distal band worn around the user's forearm as shown in Fig. 2.1. One servo motor is mounted onto the anterior side of the socket and is connected through cables to the anterior sides of the bands. The other servo motor is mounted on the posterior side of the socket and is connected through cables to the posterior sides of the bands. Feedback is generated by activating the motors to pull on the anterior or posterior sides of the proximal and distal bands in proportion to the command signal sent to the DC motors controlling the anterior and posterior tendon cables. In this way, the user is provided haptic information regarding the amount of tension in the respective actuator tendon cables.

EMG signals were recorded from the wrist flexor and extensor muscle groups of the right forearm using a Delsys Bagnoli 16-channel EMG system with two surface electrodes and a ground electrode on the elbow. EMG calibration, normalization, and offset methods are consistent with those in [39] and are briefly described in Section 4.0.2.1 below.

The two DC actuator motors were driven by a 3.5A linear current amplifier (Quanser AMPAQ-L4) with an amplification of 1V/A. Data acquisition and control were implemented through a Quanser Q8-USB data acquisition board(DAQ) operating at a 1 kHz sample rate. The whole system is controlled by a Dell Precision T5810 desktop running MATLAB R2017a. The Simulink Desktop Realtime Envi-

ronment works in conjunction with Quanser's QUARC realtime block set. The final device weighs 1.75Kg in total.

Chapter 3

Controller Design and Selection

3.0.1 Control Strategies

Terminal device flexion and extension were controlled by flexion and extension EMG signals under one of two control strategies, ALPHA or BETA. For both control strategies, EMG signals from the flexor muscles control activation of the actuator motor on the anterior sides of the prosthetic socket. Similarly, EMG signals from the extensor muscles control activation of the actuator motor on the posterior side of the prosthetic socket.

Controller ALPHA was designed to lower the effort of sustaining EMG signals while manipulating objects. In this trigger-based scheme, only a quick EMG spike of the desired magnitude is needed to proportionally activate the actuator motor. Likewise, a second EMG spike from the same muscle deactivates the actuator

motor. Thus, the user can easily control flexion and extension separately while also maintaining the ability to activate both actuators and modulate the terminal device's impedance. The control law governing flexion and extension in the ALPHA control scheme is:

$$M_{flex} = \begin{cases} max(S_{flex\,off} \cdot K_{flex\,A}),\ \gamma_{flex} = 1 \\ 0,\ \gamma_{flex} = 0 \end{cases} \tag{3.1}$$

$$M_{ext} = \begin{cases} max(S_{ext\,off} \cdot K_{ext\,A}),\ \gamma_{ext} = 1 \\ 0,\ \gamma_{ext} = 0 \end{cases} \tag{3.2}$$

Where $S_{flex\,off}$ and $S_{ext\,off}$ are the normalized offset EMG signals, $K_{ext\,A}$ and $K_{flex\,A}$ are the proportional gains of the controller, and γ_{ext} and γ_{flex} are binary variables whose value changes only if $S_{ext\,off}$ or $S_{flex\,off}$ respectively go from a negative to positive value.

Fig. 3.3a shows a signal flow diagram describing the behavior of controller ALPHA. Here, U_p and U_p^2 describe the max function in (3.1) and (3.2) and γ is depicted as a switch. In addition, the motor command signals are saturated to control the minimum and maximum current sent to the motors, ensuring the device will not draw too much current from the amplifier. Fig. 3.1 provides an illustration of the controller behavior.

Controller BETA was designed to provide more intuitive control of the prosthe-

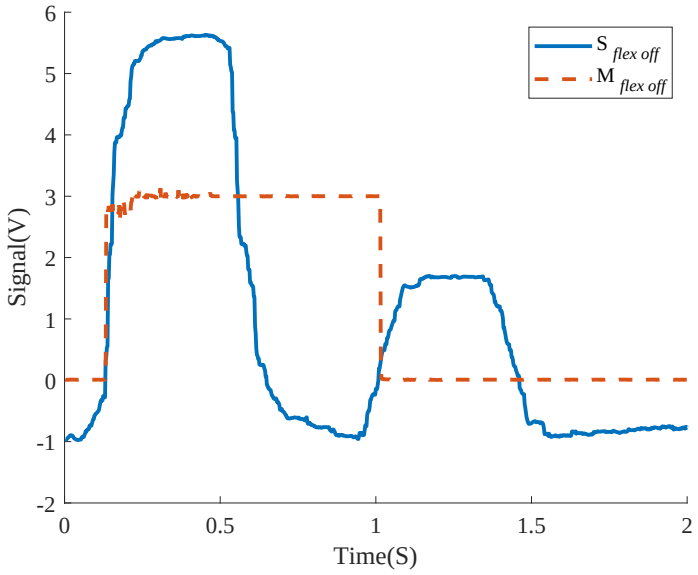

Figure 3.1: An example plot of the flexor EMG signal $S_{flex\,off}$ and the corresponding motor command signal M_{flex} for controller ALPHA © 2020 IEEE.

sis. In this scheme, each motor output is proportional to the maximum respective EMG signal recorded while that EMG signal is above zero. When both EMG signals drop below their respective relaxation thresholds, both motors relax. Thus, the user can antagonistically activate both actuators by simultaneously flexing, extending, and maintaining at least one EMG signal above the relaxation threshold. The control law governing flexion and extension in the BETA control scheme is

$$M_{flex} = \begin{cases} max(S_{flex\,off} \cdot K_{flex\,B}),\ \mathrm{S}_{flex\,off} > 0 \\ 0,\ S_{ext\,off} < T_{ext}\ \&\ S_{flex\,off} < T_{flex} \\ M_{flex,prev},\ otherwise \end{cases} \tag{3.3}$$

$$M_{ext} = \begin{cases} max(S_{ext\,off} \cdot K_{ext\,B}),\ \mathrm{S}_{ext\,off} > 0 \\ 0,\ S_{ext\,off} < T_{ext}\ \&\ S_{flex\,off} < T_{flex} \\ M_{ext,prev},\ otherwise \end{cases} \tag{3.4}$$

where $S_{flex\,off}$ and $S_{ext\,off}$ are the normalized offset EMG signals, $K_{flex\,B}$ and $K_{ext\,B}$ are the proportional gains of the controller, and T_{flex} and T_{ext} are the relaxation thresholds.

Fig. 3.3b shows the signal flow diagram describing the behavior of controller BETA. Here U_p and U_p^2 describe the max function in (3.3) and (3.4). In addition, the motor command signals are saturated as with controller ALPHA. Fig. 3.2 provides an illustration of the controller behavior.

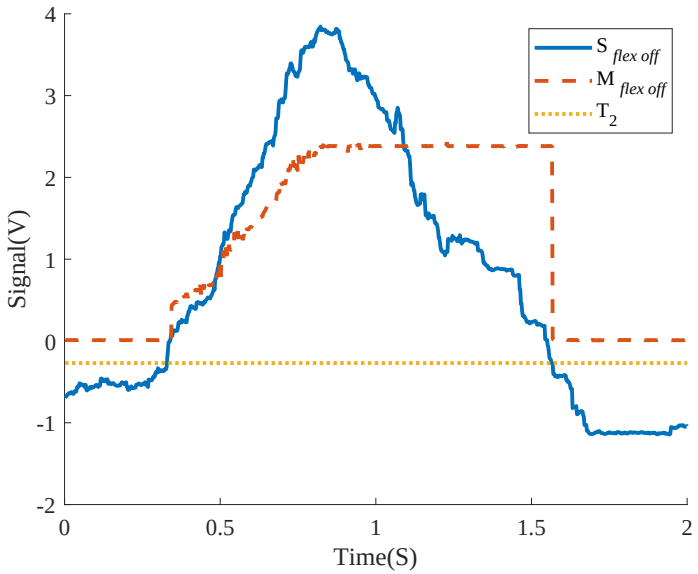

Figure 3.2: An example plot of the flexor EMG signal $S_{flex\,off}$ and the motor command signal M_{flex} for controller BETA. Note, the extensor EMG signal $S_{ext\,off} < T_{ext}$. © 2020 IEEE

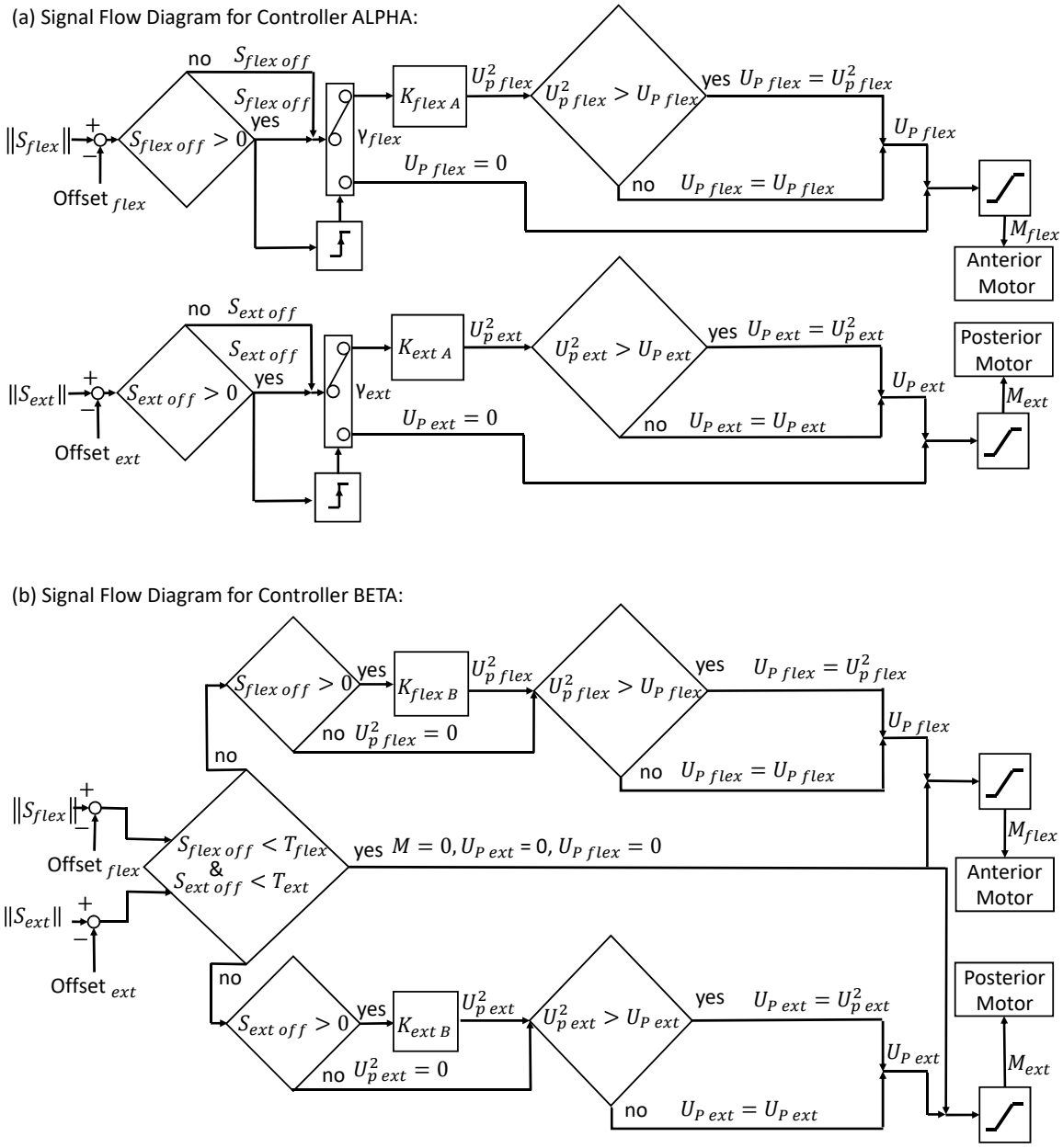

Figure 3.3: The signal flow diagrams for the two control strategies, ALPHA (a) and BETA (b) © 2020 IEEE.

3.0.2 Experimental Procedure

To evaluate the utility of each control strategy, we investigated the ability of N=6 able-bodied participants (five male, one female) ages 27.5 ± 11 (all participants above 18) to perform the Box and Blocks test [40]. This test is often used to assess manual dexterity in individuals with neurological disorders [40] and has been used to assess prosthesis function as well [41–44]. The duration of the experiment was approximately 60 minutes and participants were compensated at a rate of $10 per hour. All participants were consented according to a protocol approved by the Johns Hopkins School of Medicine Institutional Review Board (Study# IRB00147458). Participants were randomized into two groups (A and B). Participants in group A performed the task with controller ALPHA followed by controller BETA. Participants in group B performed the task with controller BETA followed by controller ALPHA. For this experiment, no haptic feedback was provided [45].

3.0.2.1 Setup and Training

After providing informed consent, participants sat on a stool facing a table where the experiment would take place. One electrode was placed over the participant's right wrist flexor muscle group and another electrode was placed over the right wrist extensor muscle group. The optimal location in these muscle groups

was located by palpating the participant's forearm while they flexed and extended their wrist. A ground electrode was then placed over the participant's right elbow. A compression sleeve covered the participant's right arm to keep the electrodes from shifting. Medical tape was gently wrapped around participant's bicep and the wires to prevent tugging.

Participants were then asked to hold their arm in the air for calibration. After a two second baseline reading, participants were asked to flex and relax their wrist in one second intervals for eight seconds while the system calibrated the minimum, maximum, and offset values for the flexor EMG signal $S_{flex\,off}$. This was then repeated for wrist extension to calibrate the extensor EMG signal $S_{ext\,off}$. Participants were instructed on the best practices for producing clear EMG signals. When controlling the prosthesis, the raw EMG signals were rectified and smoothed by taking the RMS over a 200 ms window. Additionally, the signals were normalized and offset to provide the desired input to the controller.

After calibration, participants were then informed of the control method they would be using first (based on group randomization). Participants were then instructed to place their right arm in the prosthetic socket. Additional manual adjustment was used to fine tune parameters until participants were able to repeatedly flex and extend the prosthesis with low, medium, and high tension and participants felt comfortable with the device's response to their EMG commands. Once appropriate control was achieved, participants were provided instructions on perfor-

mance of the Box and Blocks test. Then, as practice, participants were instructed, without time constraint, to move five blocks over the barrier and release them into the second compartment as seen in Fig. 3.4. If needed, further adjustment of parameters was performed.

Figure 3.4: Experimental setup of Box and Blocks test © 2020 IEEE.

3.0.2.2 Protocol

Following setup and training, participants performed eight trials of the Box and Blocks test using their designated controller. In each trial, participants were given 60 seconds to move as many blocks as possible from the right compartment of the task to the left. Participants were given a 45 second rest between each trial

and were allowed more rest time upon request. Before the first trial and after each consecutive trial, participants were asked to rank their arm fatigue on a scale from one to ten, with ten corresponding to the inability to move their arm. After completing eight trials with the first controller, participants were given time to rest while they completed a short survey regarding their perception of the controller and their ability to move blocks. Then the control method was switched to the opposite controller. Some additional manual adjustment of parameters was performed to ensure adequate control. Participants then practiced once again by moving 5 blocks over the barrier. After practice, participants were asked to rank their fatigue and allowed to rest until it returned to within one point of their previous baseline from the first controller. Participants performed eight trials of the task with the new controller using the same rest intervals. Fatigue scores were recorded after each trial. After completing the second set, participants were asked to fill out the remainder of the survey regarding their perception of the second controller, their ability to move blocks with the controller, a demographic survey, and a final survey question asking them to compare how intuitive the two controllers were. Finally, participants were given time to add any additional comments about their experience.

3.0.3 Metrics and Statistical Analysis

The two quantitative metrics used in this study to evaluate the two controllers include the block transfer rate and the block transfer efficiency. The block transfer

rate is calculated as the number of blocks moved in the 60-second trial. The block transfer efficiency is calculated as the number of blocks moved per total sum of terminal device flexions and extensions in the 60-second trial as described in

$$\eta = B_{rate}/(N_{flex} + N_{ext}) \tag{3.5}$$

Where η is the block transfer efficiency, B_{rate} is the block transfer rate, and N_{flex} and N_{ext} are terminal device flexions and extensions in the 60-second trial, respectively. In addition, survey responses for fatigue and participant's controller preference were used for qualitative assessment.

Statistical analysis was carried out in MATLAB 20184a. First, data sets were tested for normality, homogeneity of variance, and sphericity using the Lilliefors test, the Bartlett test, and the Mauchly's test, respectively. A Wilcoxon Signed-Rank test was used on the block transfer efficiency, the block transfer rate, and the survey data along with fatigue scores to determine the differences between ALPHA and BETA. Both p values and effect sizes (r) are reported when possible.

3.1 Results

All data was analyzed using non-parametric statistical analyses given the non-normal distribution ($p<.05$ for Lilliefors test). During experimentation, the experimental apparatus malfunctioned on four trials. When this occurred, the device and

task were reset and the trial was rerun. These malfunctions only affected participants two and three. In addition, participant five noted in their survey that they significantly changed their block grasping and moving strategy to improve performance in the last trial while using controller ALPHA which significantly increased their performance compared to prior trials.

3.1.1 Block Transfer Rate

Overall, the Wilcoxon Signed-Rank test showed participants moved significantly more blocks per minute with controller BETA than with controller ALPHA (p = 3.20e-08, r = -0.80) (see Fig. 3.5). Participants moved an average of 6 ± 3.49 blocks per minute when using controller ALPHA and an average of 11 ± 2.37 per minute with controller BETA.

3.1.2 Block Transfer Efficiency

Overall, the Wilcoxon Signed-Rank test showed participants were significantly more efficient with controller BETA than with controller ALPHA (p = 2.27e-08, r = -0.81) as seen in Fig. 3.6. The average block transfer efficiency for controller ALPHA was 0.22 ± 0.15, and the average block transfer efficiency for controller BETA was 0.41 ± 0.13.

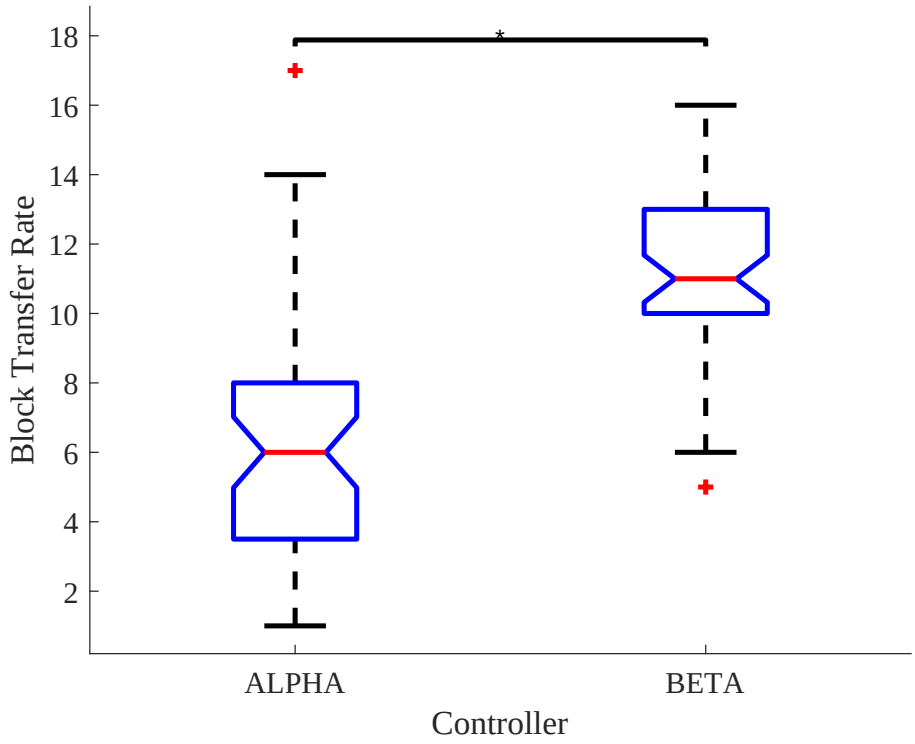

Figure 3.5: Box plot of Box and Blocks test results for controllers ALPHA and BETA. * indicates $p < 0.05$ © 2020 IEEE.

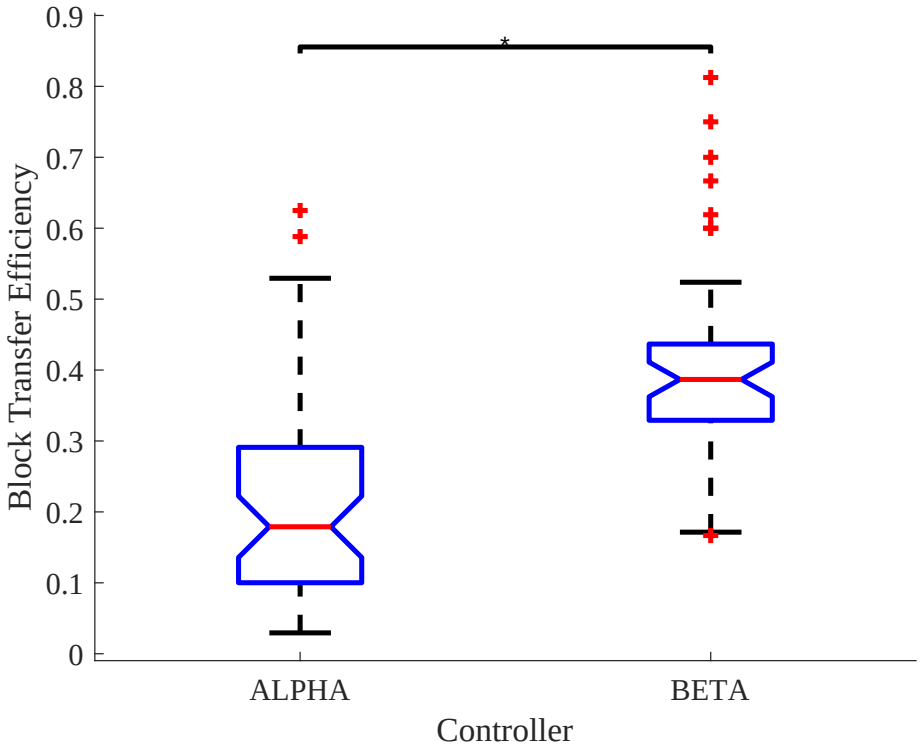

Figure 3.6: Box plot of efficiency results for controllers ALPHA and BETA.* indicates $p < 0.05$ © 2020 IEEE.

3.1.3 Survey

The Wilcoxon Signed-Rank test showed participants expressed significantly lower fatigue levels while using controller BETA than they did with controller ALPHA (p value = 0.022, r = 0.33). Additionally, the Wilcoxon Signed-Rank test showed participants overall preferred controller BETA and felt more confident in their ability to move blocks when using controller BETA (p= 0.0015). All participants but one found controller BETA to be more intuitive.

Chapter 4

Haptic Feedback

In addition to the anthropomorphic control strategy, the anthropomorphically-driven prosthesis was designed to incorporate skin stretch haptic feedback of the tension in the actuators. In this second experiment, the effects of providing haptic feedback of the tensions in the antagonistic tendons are evaluated using the same the Box and Blocks manual dexterity test described in Chapter 3 (3.0.2.1). In this way, we can evaluate the utility of haptic feedback using the same approach used to investigate the utility of the two differing control approaches.

4.0.1 Haptic Feedback Conditions

The three feedback conditions used in the second experiment were vibration feedback, skin stretch feedback, and no feedback (control). Under the no feedback condition, participants performed the Box and Blocks test using only visual cues.

For vibration feedback, two engineering acoustics C2 vibration tactors were controlled using proportional signals from the control model in Simulink to vary the magnitude of vibration. Simulink communicated with the Quanser Q8-USB data acquisition board(DAQ) which sent analog signals to a class D amplifier (Adafruit 20W Stereo Audio Amplifier - MAX9744), which converted signals into vibration commands for the tactors. The vibration frequency was held constant at 250Hz [46]. Feedback was provided such that when the anterior or posterior motor tendons were actuated, a vibration with proportional magnitude was activated on the anterior or posterior side of the participant's right bicep respectively as shown in

$$V_{flex} = M_{flex} * sin(250 * t) \tag{4.1}$$

$$V_{ext} = M_{ext} * sin(250 * t) \tag{4.2}$$

Where V_{flex} and V_{ext} are the signals sent to the Vibration motors over time t, and M_{flex} and M_{ext} are the motor commands to the anterior and posterior motors respectively as described in Chapter 3, Section 3.0.1. The skin stretch feedback was provided via the built-in haptic feedback system previously described in Section 2.0.1.2 of Chapter 2. The anterior and posterior servo motors are programmed to rotate proportionally with the motor commands sent to the corresponding anterior and posterior tendon motors. In this way participants receive a proportional skin stretch sensation over their forearm inside of the socket as they actuate the device.

4.0.2 Experimental Procedure

To evaluate the effects of providing haptic feedback to participants, we investigated the ability of N=3 able-bodied participants (two female, one male) ages 24 ± 2 to perform the Box and Blocks test [40]. This Study was a preliminary study that will inform the future direction of this research. The experiment was approximately 60 minutes in length and participants were compensated at a rate of $10 per hour. All participants were consented according to a protocol approved by the Johns Hopkins School of Medicine Institutional Review Board (Study# IRB00147458). Participants were randomized into one of six groups which differed with respect to the condition order. Subject one was presented with the skin stretch feedback first, no feedback second, and vibration feedback last. Subject two was presented with skin stretch feedback first, vibration feedback second, and no feedback last. Subject three was presented with no feedback first, skin stretch feedback second, and vibration feedback last. Under all conditions, participants wore noise cancelling headphones to reduce auditory feedback effects from the vibration motors and from the servo motors.

4.0.2.1 Setup and Training

After providing informed consent, participants sat on a stool facing a table where the experiment would take place. The first portion of the survey regarding

participant demographics was administered. One EMG electrode was placed over the participant's right wrist flexor muscle group and another electrode was placed over the right wrist extensor muscle group. The optimal electrode location was determined by palpating the participant's forearm while they flexed and extended their wrist. A ground electrode was then placed over the participant's right elbow. A compression sleeve covered the participant's right arm to keep the electrodes from shifting. Medical tape was gently wrapped around participant's bicep and the wires to prevent tugging.

Participants were then asked to hold their arm in the air for the first of two calibrations. After a two second baseline reading, participants were asked to flex and relax their wrist in one second intervals for eight seconds while the system calibrated the minimum, maximum, and offset values for the flexor EMG signal $S_{flex\,off}$. This was then repeated for wrist extension to calibrate the extensor EMG signal $S_{ext\,off}$. Participants were instructed on the best practices for producing clear EMG signals.

Participants then completed an EMG evaluation exercise. In the task, participants were instructed to watch a monitor that was placed in front of them and displayed a simulink virtual environment containing two circles. One white circle approximately one inch diameter centered over a second red circle of the same size approximately three inches below. Participants were informed that extending their wrist would move the red ball to the right and flexing their wrist would move

the red ball to the left. They were asked to keep the red ball in line with the white ball as best as they could for two 30-second practice sessions. Participants were also informed that the white ball would move to the right first to eliminate large differences between participants. After a five second count down, the white ball moved in a sinusoidal pattern for 30 seconds for each of the two trajectories.

$$P = 2sin(t) \tag{4.3}$$

$$P = \frac{4}{3}sin(\frac{t}{3}) + \frac{4}{3}sin(\frac{4t}{3}) \tag{4.4}$$

where P is the position of the white ball relative to the time t. Equation 4.3 was intended to be easier than equation 4.4 as equation 4.3 was presented first. Sinusoidal frequency and complexity were adjusted to be reasonable and adequate for the difficulty level. A higher frequency and more complex signal was intended to be more difficult. Times were displayed on the monitor for participants to see. The task display can be seen in Fig. 4.1.

Participants were then fitted into the prosthetic device with skin stretch bands properly tightened and vibration motors were placed over the anterior and posterior sides of the participants' right bicep. After a second EMG calibration with their arm in the prosthetic socket, participants were informed of the control method they would be using (controller BETA is described in Section 3.0.1 of Chapter 3).

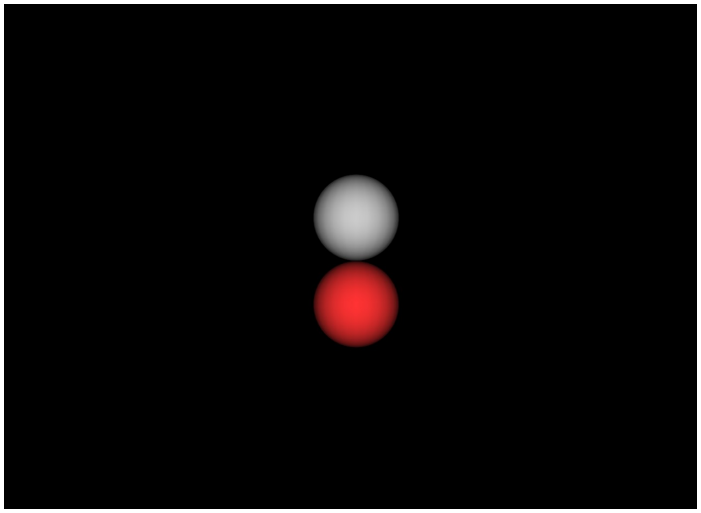

Figure 4.1: EMG training task screen before task begins

Additional manual adjustment was used to fine tune parameters until participants were able to repeatedly flex and extend the prosthesis with low, medium, and high tension and participants felt comfortable with the device's response to their EMG commands. Once appropriate control was achieved, participants were provided instructions on performance of the Box and Blocks test. Then, as practice, participants were instructed, without time constraint, to move five blocks over the barrier and release them into the second compartment. If needed, further adjustment of parameters was performed here.

In order to provide participants with practice under each condition, participants performed a 30-second trial of the Box and Blocks test under each condition in the following order: no feedback, vibration feedback, and skin stretch feedback.

4.0.2.2 Protocol

After setup and training was complete, participants performed four of the Box and Blocks test under each condition in the order that had been randomly assigned to them. In each trial, participants were given 60 seconds to move as many blocks as possible from the right compartment of the task to the left (from the participants' perspective). Participants were given a 45 second rest between each trial and were allowed more rest time upon request. After completing four trials with the first condition, participants were given time to rest while they completed a short survey regarding their perception of the controller and their ability to move blocks. Then the haptic feedback condition was switched to the next assigned feedback modality. Participants then performed four trials of the task under the new condition using the same rest intervals. After completing the second set, participants were given time to rest while they filled out the second portion of the survey regarding their perception of the condition and their ability to move blocks under the second condition. Next, the haptic feedback condition was switched to the last assigned feedback modality. Participants then performed four trials of the task under the new condition using the same rest intervals. After completing the last set of trials, participants were given the last portion of the survey regarding their perception of the condition and their ability to move blocks under the last condition as well as a two questions regarding their overall perception of their performance and of the ease of use of the conditions. Finally, participants were given time to add any

additional comments about their experience.

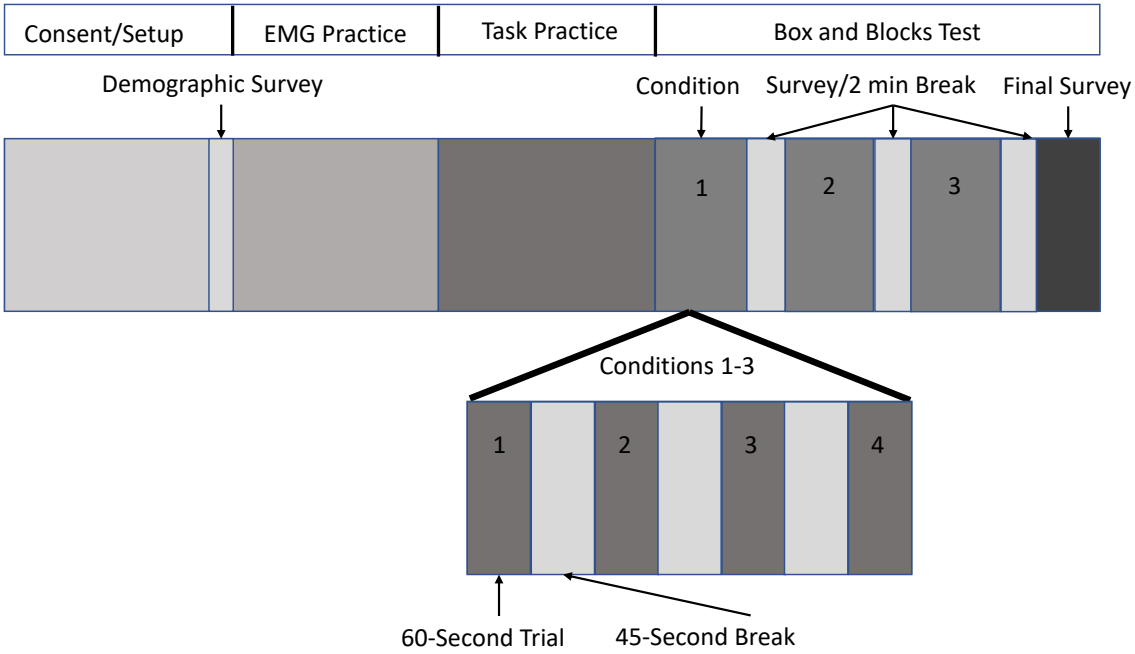

Figure 4.2: Experiment 2 protocol layout in block format

4.0.3 Metrics and Statistical Analysis

Two quantitative metrics were used in this study to evaluate the effect of haptic feedback, block transfer rate and block transfer efficiency. The block transfer rate is calculated as the number of blocks moved in the 60-second trial. The block transfer efficiency is calculated as the number of blocks moved per total sum of terminal device flexions and extensions in the 60-second trial just as in Section 3.0.3 Chapter 3.

Statistical analysis was carried out in R 3.6.1. Data sets were tested for normal-

ity using the Lilliefors test. As data sets were normal, a linear mixed-effects model was used to model the block transfer rates and the block transfer efficiency with fixed effects for condition and trial number as well as random effects for subject. Bonferrioni corrections were used on p-values as there were multiple comparisons for the data set. A p-value of 0.05 was used as the threshold for significance.

4.0.4 Results

During experimentation, the experimental apparatus malfunctioned on four trials. When this occurred, the device and task were reset and the trial was rerun. These malfunctions only happened with participants two and three and did not affect their results.

4.0.4.1 Block Transfer Rate

Overall, the linear mixed-effects model of the block transfer rate test data had a significant effect of intercept (p = 0.0325). The model showed that there were significant learning effects across the no haptic feedback trials (estimate = 0.7483, p = 0.00639). However the mixed-effects model showed no significant difference in block transfer rate between the no feedback condition and either of the haptic feedback conditions ($p>0.1$ for all comparisons). Results of participant performance are shown in Fig. 4.3.

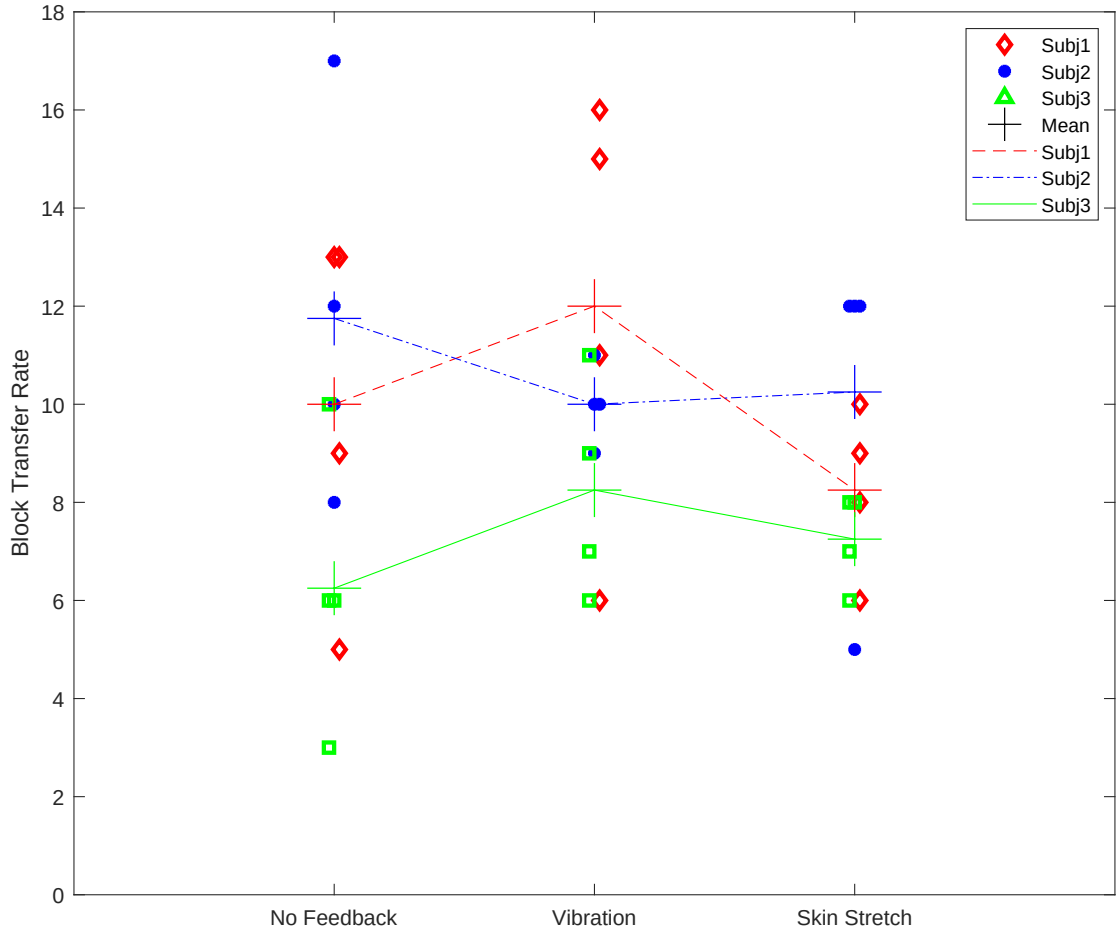

Figure 4.3: Block transfer rate data with lines between subject means for each condition

4.0.4.2 Block Transfer Efficiency

Overall, the linear mixed-effects model of the block transfer efficiency data had a significant effect of intercept (p = 0.02556). The model showed significant learning effects across trials for the no feedback condition (estimate = 0.0049185). Additionally, the mixed-effects model showed no significant difference in block transfer efficiency between the no feedback condition and either of the haptic feedback conditions. Results of participant efficiency are shown in Fig. 4.4.

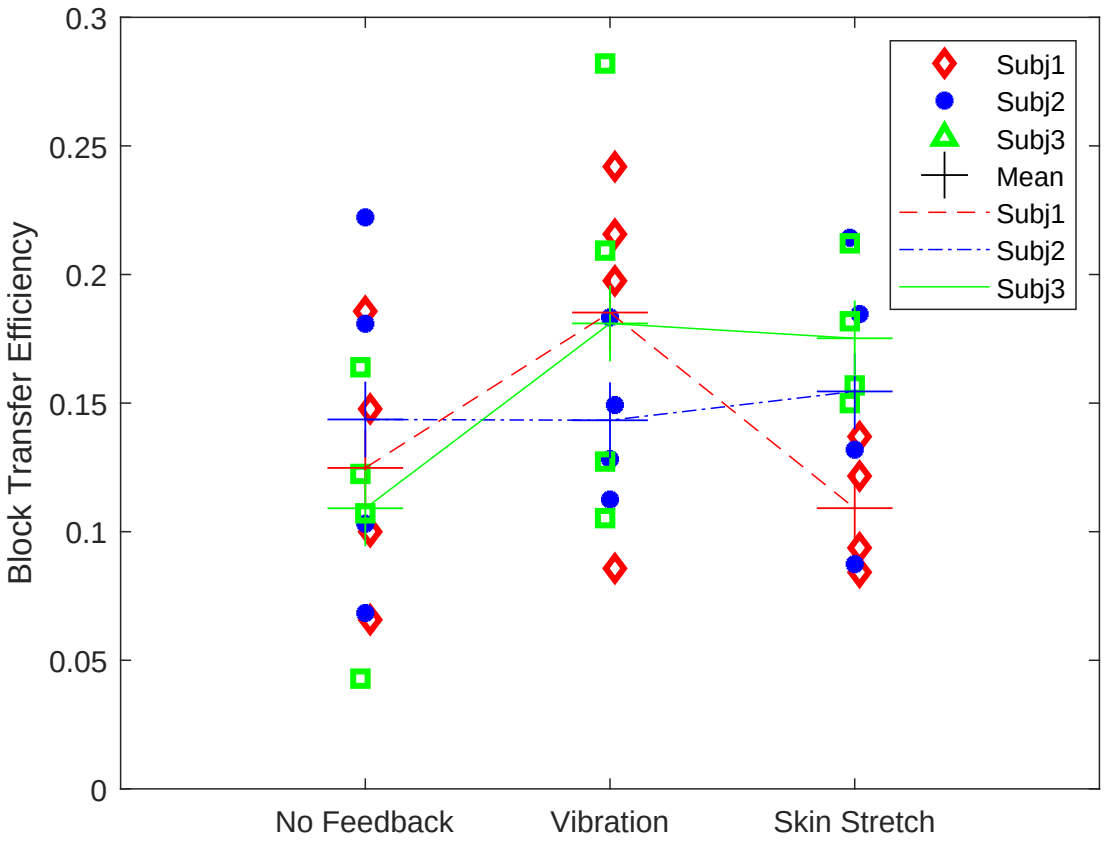

Figure 4.4: Block transfer Efficiency data with lines between subject means for each condition

Chapter 5

Discussion

In this study, we presented the development of an anthropomorphically-driven prosthesis that features a tension-based haptic feedback system and the results of two small user studies designed to evaluate prosthesis function and usability. The first study investigated two competing control strategies for the prosthesis. The second study evaluated the effect of haptic feedback on participants' task performance with the prosthesis.

In the first experiment it was shown that controller BETA allowed for better task performance than controller ALPHA both in terms of the block transfer rate and the block transfer efficiency, and was participants' preferred control strategy. The superiority of controller BETA is likely due to its intuitive nature, where muscle signals correspond more directly with motor control. Despite the fact that controller ALPHA allowed participants to relax their EMG signals, participants reported less

fatigue with controller BETA than with controller ALPHA. Thus, controller BETA seems to stand out as a more effective way to control this device.

Based on the results from the first experiment, controller BETA was chosen as the controller used in the second experiment under all feedback conditions. Results from the second experiment, while incomplete, still provide a number of valuable insights. First, all participants showed learning effects across their no haptic feedback condition trials. It is possible that training periods were not sufficient to reduce these effects or that instruction on how to use the prosthesis to perform the task should be provided. Alternatively, it is possible that since these effects were only present in the no feedback condition that providing haptic feedback allowed for reduced learning effects.

5.0.1 Task Performance

It is also worth considering how task performance with this prosthesis compares to task performance with other prostheses and prosthesis control schemes. Table 5.1 highlights the average Box and Blocks test scores from participants using their dominant right hand as well as various clinical prostheses. The table also includes data from some able bodied subjects as well as some amputees. Note, some scores have been adjusted to reflect the 1 minute trials used in these studies. These averages are results from the first experiment described in Chapter 3. Results for the device with haptic feedback are not presented as the data set is

incomplete and the presentation would be premature.

Table 5.1: Table of Reported Box and Blocks scores Reported Box and Blocks scores for various types of prostheses © 2020 IEEE.

Conditions	Blocks per Minute	Source
Female dominant right hand	86 ± 7.4	[40]
Custom body-powered prosthesis	$15 - 20$	[41]
Standard myoelectric prosthesis	$\approx 3 \pm 2.5^{**}$	[42]
TMR* prosthesis	$\approx 8 \pm 4.5^{**}$	[42]
Hosmer hook prosthesis	22.7	[43]
Michelangelo prosthesis	29.3 ± 3.20	[44]
ALPHA (this manuscript)	6 ± 3.49	N/A
BETA (this manuscript)	11 ± 2.37	N/A

*Targeted muscle reinnervation ** Approximated from graphic

While the training periods and number of trials vary for the Box and Blocks test scores reported in Table 5.1, these scores provide insight into the current level of manual dexterity in prostheses. Our anthropomorphically-driven prosthesis resulted in higher mean scores than some records for standard myoelectric prostheses with both controllers (ALPHA and BETA). Additionally, under controller BETA, participants with this anthropomorphically-driven prosthesis also scored higher on average than some targeted muscle reinnervation prosthesis users. At the same time, the Michelangelo prosthesis seems to greatly outperform any other prosthesis, likely due, at least in part, to the six months of training provided to the participants. Body-powered prostheses also tend to outperform myoelectric prostheses. This is likely due to the high fidelity control they provide in addition to the inherent haptic feedback provided to the amputee. It is possible that the scores for our anthropomorphic prosthesis might improve with extended training periods and with

the haptic feedback engaged.

5.0.2 Limitations

While these results show promise for anthropomorphically-driven prostheses, the current device has limitations that should be addressed. First, despite its wearability, the device is highly cumbersome. The weight of the motors and the need for precise EMG signals can be mentally and physically exhausting. Participants reported high fatigue scores very early in experiment 1 and many participants left comments about how they felt the device was heavy. This likely affected their performance throughout the trials from both a physical and cognitive perspective.

Second, participants had different arm sizes and the custom socket did not fit all participants snugly, even with the compression sleeve used to adjust the fit. This caused the device to slightly shift on their arms as they performed the task. This can likely also affect the way participants were sensing the skin stretch haptic feedback.

Third, some participants had a difficult time sensing the skin stretch while actively moving the arm. With the amount of sensory overload occurring over the surface of their forearm, it is possible the feedback is lost in the sensation of wearing the socket. Perhaps this provides some insight into the utility of building haptic feedback into prosthesis sockets. A future study comparing the differences in perception between the skin stretch feedback being displayed inside the socket or

outside the socket could clarify the effects of this confound in the study.

Finally, only able-bodied participants were tested in this experiment. The device is currently designed to work with able-bodied participants but could be modified to attach to an amputee's socket in future experiment utilizing the Hosmer quick disconnect at the wrist. Additionally, the actuation motors could be temporarily fastened to a different socket.

5.0.3 Future Directions

Based on these results and limitations, the next iteration of this study should include the following adjustments. First, the vibration motors should be fixed to reduce the interference with the EMG control. Second, the opposable thumb should be remodeled to allow for better grip patterns and to prevent the middle finger from catching on the thumb. Based on the results and experience from the second experiment, it may also be beneficial to redesign the built-in haptic feedback system to reduce haptic stimulation from the socket and increase the force produced by the built-in feedback.

Third, it may be beneficial to have extended training periods. While providing more training may cause user fatigue to rise, the reduction of training effects in the experiment will likely improve user performance, reduce within subject variance, and aid in clarifying the effects of the haptic feedback on task performance. However, it may also be beneficial to run the study again with short training periods in

order to allow for differences in training effects to be highlighted. This may provide insight into potential effects of providing feedback on reducing training effects.

Finally, subsequent studies investigating the anthropomorphically-driven prosthesis could use different tasks, such as an activity of daily living task, to asses the device and the role of haptic feedback in its function. This would allow for a more realistic scenario in which to test the device. In addition, this could be an ideal way of including amputees in the participant pool.

Overall, these experiments have established a framework for future exploration of haptics in anthropomorphically-driven prostheses. While the findings presented here are preliminary, they provide pertinent insight needed to conduct future studies on this topic. Furthermore, information regarding the utility of haptics may provide insight for future studies with brain machine interfaces (BMI) that include prostheses. By knowing the precise utility of various forms of haptics in using prostheses, future BMI studies will be able to discern if it is necessary to use haptic feedback channels to provide information such as tension for anthropomorphically-driven prostheses. In addition, the design of this wearable anthropomorphically-driven prosthesis is unique and offers useful simplifications to improve wear-ability. This project opens the next step for anthropomorphically-driven prostheses to move from purely experimental devices to becoming available to amputees. Prosthetic devices are advancing at a rapid pace in control, design, and haptic feedback. Each new design, while not yet ideal in form or function, provides hope that future

iterations will provide amputees with a truly useful biomedical device.

Appendix A

Device Maintenance

A.0.1 Running the Device

The Following describes how to turn the system on and how to run the Anthropomorphically driven prosthesis.

Turn on Dell computer at prosthesis work station under the double layered desk that is just to the right when you enter Kriger 60.

Turn on the power-strip that is built into the double layered desk on the inside of the right arm supporting the second layer of the desk. the switch will glow red when the power strip is on.

Turn on the black power-strip on the prosthesis desk in the front right corner of the room from when you enter K60. A red Light will turn on with the power strip.

Turn on the liner current amplifier (Quanser AMPAQ-L4) (a black box with the

switch on the back of the device) on the prosthesis desk in the front right corner of the room from when you enter K60. The amplifier should start to hum and and lights should turn in the front. Check that the lights are green for the 1st and 2nd channels.

To Run the built in haptics: turn on the Demo Box Described in Appendix B

A.0.2 Device Troubleshooting

Throughout the design and use of the anthropomorphically-driven prosthesis, a number of potential failure modes have been exposed. First and foremost, the 3D printed hand's guide loops are in a high wear environment and should be monitored to prevent unexpected breakage. If a section seems worn, a replacement piece should be printed and installed. In addition, both the finger tendon cables and actuator cables are in high strain environments. While failure is more sudden with these cables, the devices should be stopped if any cable breaks and a replacement should be installed.

Actuation cables are bound to the actuator DC motors by press fit shaft couplers and friction cloth. If the motor spins freely but the actuation cable has not broken then the coupling has likely failed. Replace the actuation cable and the friction cloth as they have likely become worn.

In the case that either DC actuator motor or servo motor should malfunction, check RCA cables for circuit breaks and that the motor amplifier's fuse is intact. If

RCA cables are working, the fuse is intact and the motors will not run, a replacement component should be installed.

A.0.3 Components List

Table A.1: Table of Components in the Wearable Anthropomorphically-Driven Prosthesis

Component	Details	Source
DC Motor	RE 30 Ø30 mm, Graphite Brushes, 60 Watt	Maxon
Actuator Tendon Cable	50lb Fishing Line	Amazon
Finger Tendon Cables	33 Pound 0.6mm Fishing steel Wire Nylon Coated	Amazon
Cable Crimps	Double Barrel Crimp Sleeves .6mm x 7mm	Amazon
Stainless Steel Ball Bearing	Flanged, Shielded, NO. 695-2Z, for 5 mm Shaft Diameter	McMamster-carr
Motor Shaft Collar	for 6 mm Diameter, 2024 Aluminum 9mm width	McMamster-carr
Restorative Spring	N/A	N/A
Servo Motors	MG90D High Torque Metal Gear	Adafruit
Haptic Bands	N/A	Amazon
Vibration Tactors	C-2 Tactor with 200-300 Hz Range	Engineering acoustics
Vibration Tactor Amplifier	Stereo 20W Class D Audio Amplifier - MAX9744	Adafruit
RCA Cables	N/A	Amazon
Blocks	1 Inch cube Model:9505X	Amazon

* **

Appendix B

Device Demonstration

In order to demonstrate the built-in haptic feedback system of the anthropomorphically-driven prosthesis during demonstrations, the control system can be simplified from myoelectric control to manual control using two rotary dials that separately control the anterior and posterior actuation of the prosthesis. The control box, shown in Fig. B.1, is used to increase the tension in the anterior and posterior cables of the prosthesis. They will also be allowed to turn the haptic feedback on and off so that they can better understand the utility of the haptic feedback system. In this way, the system can demonstrate the repercussions of sensory deprivation that comes with many types of neuroprostheses.

Figure B.1: Control Module Control module for prosthesis and haptic feedback

Bibliography

[1] A. Sabzi Sarvestani and A. Taheri Azam, “Amputation: A Ten-Year Survey,” *Trauma Monthly*, vol. 18, no. 3, pp. 126–129, dec 2013.

[2] C. Toledo, L. Leija, R. Munoz, A. Vera, and A. Ramirez, “Upper limb prostheses for amputations above elbow: A review,” in *2009 Pan American Health Care Exchanges*, 2009, pp. 104–108.

[3] F. Cordella, A. L. Ciancio, R. Sacchetti, A. Davalli, A. G. Cutti, E. Guglielmelli, and L. Zollo, “Literature Review on Needs of Upper Limb Prosthesis Users,” *Frontiers in Neuroscience*, vol. 10, aug 2016.

[4] M. T. Leddy and A. M. Dollar, “Preliminary Design and Evaluation of a Single-Actuator Anthropomorphic Prosthetic Hand with Multiple Distinct Grasp Types,” in *2018 7th IEEE International Conference on Biomedical Robotics and Biomechatronics (Biorob)*, 2018, pp. 1062–1069.

[5] N. Hogan, “Adaptive control of mechanical impedance by coactivation of

antagonist muscles," *IEEE Transactions on Automatic Control*, vol. 29, no. 8, pp. 681–690, 1984.

[6] J. Buzzi, C. Gatti, G. Ferrigno, and E. De Momi, "Analysis of Joint and Hand Impedance During Teleoperation and Free-Hand Task Execution," *IEEE Robotics and Automation Letters*, vol. 2, no. 3, pp. 1733–1739, 2017.

[7] A. A. Blank, A. M. Okamura, and L. L. Whitcomb, "Task-dependent impedance and implications for upper-limb prosthesis control," *The International Journal of Robotics Research*, vol. 33, no. 6, pp. 827–846, dec 2014.

[8] J. D. Brown, A. Paek, M. Syed, M. K. O'Malley, P. A. Shewokis, J. L. Contreras-Vidal, A. J. Davis, and R. B. Gillespie, "An exploration of grip force regulation with a low-impedance myoelectric prosthesis featuring referred haptic feedback," *Journal of NeuroEngineering and Rehabilitation*, vol. 12, no. 1, p. 104, dec 2015.

[9] C. Li, X. Gu, X. Xiao, G. Zhu, A. V. Prituja, and H. Ren, "Transcend Anthropomorphic Robotic Grasping With Modular Antagonistic Mechanisms and Adhesive Soft Modulations," *IEEE Robotics and Automation Letters*, vol. 4, no. 3, pp. 2463–2470, 2019.

[10] Z. Xu, Y. Matsuoka, and A. D. Deshpande, "Crocheted artificial tendons and ligaments for the anatomically correct testbed (ACT) hand," in *2015 IEEE*

International Conference on Robotics and Biomimetics (ROBIO), 2015, pp. 2449–2453.

[11] Z. Xu and E. Todorov, “Design of a highly biomimetic anthropomorphic robotic hand towards artificial limb regeneration,” in *2016 IEEE International Conference on Robotics and Automation (ICRA)*, 2016, pp. 3485–3492.

[12] E. Battaglia, J. Clark, M. Bianchi, M. Catalano, A. Bicchi, and M. K. O’Malley, “Skin stretch haptic feedback to convey closure information in anthropomorphic, under-actuated upper limb soft prostheses,” *IEEE Transactions on Haptics*, p. 1, 2019.

[13] S. B. Godfrey, A. Altobelli, M. Rossi, and A. Bicchi, “Effect of homogenous object stiffness on tri-digit grasp properties,” in *2015 37th Annual International Conference of the IEEE Engineering in Medicine and Biology Society (EMBC)*, 2015, pp. 6704–6707.

[14] I. Williams and T. G. Constandinou, “Modelling muscle spindle dynamics for a proprioceptive prosthesis,” *Conference proceedings: ... Annual International Conference of the IEEE Engineering in Medicine and Biology Society. IEEE Engineering in Medicine and Biology Society. Annual Conference*, vol. 2013, pp. 1923–1926, 2013.

[15] A. Panarese, B. B. Edin, F. Vecchi, M. C. Carrozza, and R. S. Johansson, “Humans Can Integrate Force Feedback to Toes in Their Sensorimotor

Control of a Robotic Hand," *IEEE Transactions on Neural Systems and Rehabilitation Engineering*, vol. 17, no. 6, pp. 560–567, 2009.

[16] E. L. Graczyk, A. Gill, D. J. Tyler, and L. J. Resnik, "The benefits of sensation on the experience of a hand: A qualitative case series," *PLoS ONE*, vol. 14, no. 1, sep 2019.

[17] S. Lewis, M. F. Russold, H. Dietl, and E. Kaniusas, "User demands for sensory feedback in upper extremity prostheses," in *2012 IEEE International Symposium on Medical Measurements and Applications Proceedings*, 2012, pp. 1–4.

[18] R. S. Johansson and J. R. Flanagan, "Coding and use of tactile signals from the fingertips in object manipulation tasks," *Nature Reviews Neuroscience*, vol. 10, no. 5, pp. 345–359, apr 2009.

[19] C. Xiong, W. Chen, B. Sun, M. Liu, S. Yue, and W. Chen, "Design and Implementation of an Anthropomorphic Hand for Replicating Human Grasping Functions," *IEEE Transactions on Robotics*, vol. 32, no. 3, pp. 652–671, 2016.

[20] S. L. Carey, D. J. Lura, M. J. Highsmith, CP, and FAAOP, "Differences in myoelectric and body-powered upper-limb prostheses: Systematic literature review," *Journal of Rehabilitation Research and Development*, vol. 52, no. 3, pp. 247–262, apr 2015.

[21] A. V. Kobelev and S. I. Shchukin, “Anthropomorphic prosthesis control based on the electrical impedance signals analysis,” in *2018 Ural Symposium on Biomedical Engineering, Radioelectronics and Information Technology (USBEREIT)*, 2018, pp. 33–36.

[22] A. G. Chappell, S. W. Jordan, and G. A. Dumanian, “Targeted Muscle Reinnervation for Treatment of Neuropathic Pain,” *Clinics in Plastic Surgery*, vol. 47, no. 2, pp. 285–293, 2020.

[23] H. Myers, D. Lu, S. J. Gray, and F. Bruscino-Raiola, “Targeted muscle reinnervation to improve electromyography signals for advanced myoelectric prosthetic limbs: a series of seven patients,” *ANZ journal of surgery*, vol. 90, no. 4, pp. 591–596, 2020.

[24] K. A. Yildiz, A. Y. Shin, and K. R. Kaufman, “Interfaces with the peripheral nervous system for the control of a neuroprosthetic limb: a review,” *Journal of Neuroengineering and Rehabilitation*, vol. 17, no. 1, p. 43, 2020.

[25] A. L. Ciancio, F. Cordella, R. Barone, R. A. Romeo, A. D. Bellingegni, R. Sacchetti, A. Davalli, G. Di Pino, F. Ranieri, V. Di Lazzaro, E. Guglielmelli, and L. Zollo, “Control of Prosthetic Hands via the Peripheral Nervous System,” *Frontiers in Neuroscience*, vol. 10, apr 2016.

[26] B. P. Christie, M. Freeberg, W. D. Memberg, G. J. C. Pinault, H. A. Hoyen, D. J. Tyler, and R. J. Triolo, “”Long-term stability of stimulating spiral nerve

cuff electrodes on human peripheral nerves”,” *Journal of Neuroengineering and Rehabilitation*, vol. 14, no. 1, p. 70, 2017.

[27] M. S. Fifer, S. Acharya, H. L. Benz, M. Mollazadeh, N. E. Crone, and N. V. Thakor, “Toward Electrocorticographic Control of a Dexterous Upper Limb Prosthesis: Building Brain-Machine Interfaces,” *IEEE Pulse*, vol. 3, no. 1, pp. 38–42, apr 2012.

[28] N. V. Thakor, M. S. Fifer, G. Hotson, H. L. Benz, G. I. Newman, G. W. Milsap, and N. E. Crone, “Neuroprosthetic limb control with electrocorticography: Approaches and challenges,” in *2014 36th Annual International Conference of the IEEE Engineering in Medicine and Biology Society*, 2014, pp. 5212–5215.

[29] A. Calado, F. Soares, and D. Matos, “A Review on Commercially Available Anthropomorphic Myoelectric Prosthetic Hands, Pattern-Recognition-Based Microcontrollers and sEMG Sensors used for Prosthetic Control,” in *2019 IEEE International Conference on Autonomous Robot Systems and Competitions (ICARSC)*, 2019, pp. 1–6.

[30] A. Jackson, C. T. Moritz, J. Mavoori, T. H. Lucas, and E. E. Fetz, “The neurochip BCI: towards a neural prosthesis for upper limb function,” *IEEE Transactions on Neural Systems and Rehabilitation Engineering*, vol. 14, no. 2, pp. 187–190, 2006.

[31] S. Wendelken, D. M. Page, T. Davis, H. A. C. Wark, D. T. Kluger, C. Duncan, D. J. Warren, D. T. Hutchinson, and G. A. Clark, "Restoration of motor control and proprioceptive and cutaneous sensation in humans with prior upper-limb amputation via multiple Utah Slanted Electrode Arrays (USEAs) implanted in residual peripheral arm nerves," *Journal of NeuroEngineering and Rehabilitation*, vol. 14, apr 2017.

[32] J. Egan, J. Baker, P. House, and B. Greger, "Detection and classification of multiple finger movements using a chronically implanted Utah Electrode Array," in *2011 Annual International Conference of the IEEE Engineering in Medicine and Biology Society*, 2011, pp. 7320–7323.

[33] A. Sharma, L. Rieth, P. Tathireddy, R. Harrison, H. Oppermann, M. Klein, M. Töpper, E. Jung, R. Normann, G. Clark, and F. Solzbacher, "Evaluation of the packaging and encapsulation reliability in fully integrated, fully wireless 100 channel Utah Slant Electrode Array (USEA): Implications for long term functionality," in *2011 16th International Solid-State Sensors, Actuators and Microsystems Conference*, 2011, pp. 1204–1207.

[34] A. M. Wilder, S. D. Hiatt, B. R. Dowden, N. A. T. Brown, R. A. Normann, and G. A. Clark, "Automated Stimulus-Response Mapping of High-Electrode-Count Neural Implants," *IEEE Transactions on Neural Systems and Rehabilitation Engineering*, vol. 17, no. 5, pp. 504–511, 2009.

[35] K. Horch and G. Dhillon, “Towards a Neuroprosthetic Arm,” in *The First IEEE/RAS-EMBS International Conference on Biomedical Robotics and Biomechatronics, 2006. BioRob 2006.*, 2006, pp. 1125–1128.

[36] A. Atasoy, E. Toptas, S. Kuchimov, S. Gulfize, M. Turpcu, E. Kaplanoglu, B. Guclu, and M. Ozkan, “Biomechanical Design of an Anthropomorphic Prosthetic Hand,” in *2018 7th IEEE International Conference on Biomedical Robotics and Biomechatronics (Biorob)*. IEEE, aug 2018, pp. 732–736.

[37] J. Hendo, “3D Printed Bionic Hand Skeleton,” aug 2019.

[38] O. Kayhan, A. K. Nennioglu, and E. Samur, “A skin stretch tactor for sensory substitution of wrist proprioception,” in *2018 IEEE Haptics Symposium (HAPTICS)*, 2018, pp. 26–31.

[39] N. Thomas, G. Ung, C. McGarvey, and J. D. Brown, “Comparison of vibrotactile and joint-torque feedback in a myoelectric upper-limb prosthesis,” *Journal of NeuroEngineering and Rehabilitation*, vol. 16, no. 1, p. 70, sep 2019.

[40] V. Mathiowetz, G. Volland, N. Kashman, and K. Weber, “Adult Norms for the Box and Block Test of Manual Dexterity,” *American Journal of Occupational Therapy*, vol. 39, no. 6, pp. 386–391, dec 1985.

[41] K. D. Gemmell, M. T. Leddy, J. T. Belter, and A. M. Dollar, “Investigation of

a passive capstan based grasp enhancement feature in a voluntary-closing prosthetic terminal device," in *2016 38th Annual International Conference of the IEEE Engineering in Medicine and Biology Society (EMBC)*, 2016, pp. 5019–5025.

[42] L. A. Miller, K. A. Stubblefield, R. D. Lipschutz, B. A. Lock, and T. A. Kuiken, "Improved Myoelectric Prosthesis Control Using Targeted Reinnervation Surgery: A Case Series," *IEEE Transactions on Neural Systems and Rehabilitation Engineering*, vol. 16, no. 1, pp. 46–50, 2008.

[43] J. T. Belter, M. T. Leddy, K. D. Gemmell, and A. M. Dollar, "Comparative clinical evaluation of the Yale Multigrasp Hand," in *2016 6th IEEE International Conference on Biomedical Robotics and Biomechatronics (BioRob)*, 2016, pp. 528–535.

[44] M. Luchetti, A. G. Cutti, G. Verni, R. Sacchetti, and N. Rossi, "Impact of Michelangelo prosthetic hand: Findings from a crossover longitudinal study," *Journal of Rehabilitation Research and Development*, vol. 52, no. 5, pp. 605–618, dec 2015.

[45] E. Miller, I. Amanze, and J. Brown, "© 20XX IEEE. Reprinted, with permission, from A Wearable Anthropomorphically-Driven Prosthesis with a Built-In Haptic Feedback System."

[46] H. J. B. Witteveen, H. S. Rietman, and P. H. Veltink, "Vibrotactile grasping

force and hand aperture feedback for myoelectric forearm prosthesis users:," *Prosthetics and Orthotics International*, apr 2014.

Vita

Ethan Dominic Miller was born in Shoreham-by-Sea, England on June 26th, 1996. He has always had a great interest in developing devices that could help people. He attended the University of Louisville in Louisville, Kentucky and received his bachelors in biomedical engineering in May of 2018. He is currently finishing his masters degree in biomedical engineering from the Johns Hopkins University in Baltimore, Maryland. As a research assistant, Ethan worked in Dr. Jeremy Brown's haptics and medical robotics laboratory on exploring the utility of

unique haptics for anthropomorphically-driven prostheses. By developing a better understanding of the utility of providing haptic feedback regarding antagonistic tensions in an anthropomorphically-driven prosthesis, he hopes to improve future prostheses and provide insight into developing more useful neuroprostheses.